Construction and Building Materials 229 (2019) 116874

Contents lists available at ScienceDirect

Construction and Building Materials

journal homepage: www.elsevier.com/locate/conbuildmat

Recycling of paper sludge powder for achieving sustainable and energy-saving building materials

Mingxu Chen [a], Yan Zheng [a], Xiangming Zhou [b], Laibo Li [a], Shoude Wang [a], Piqi Zhao [a], Lingchao Lu [a,*], Xin Cheng [a,*]

[a] Shandong Provincial Key Lab. of Preparation and Measurement of Building Materials, University of Jinan, Jinan 250022, China
[b] Department of Mechanical, Aerospace and Civil Engineering, Brunel University, London, Uxbridge, Middlesex UB8 3PH, United Kingdom

HIGHLIGHTS

- The utilization of paper sludge develops energy-saving CSBM with enhanced properties.
- RSM is an effective method to predict the properties of sustainable CSBM.
- Paper sludge benefits to the development of waste management and energy efficiency.

GRAPHICAL ABSTRACT

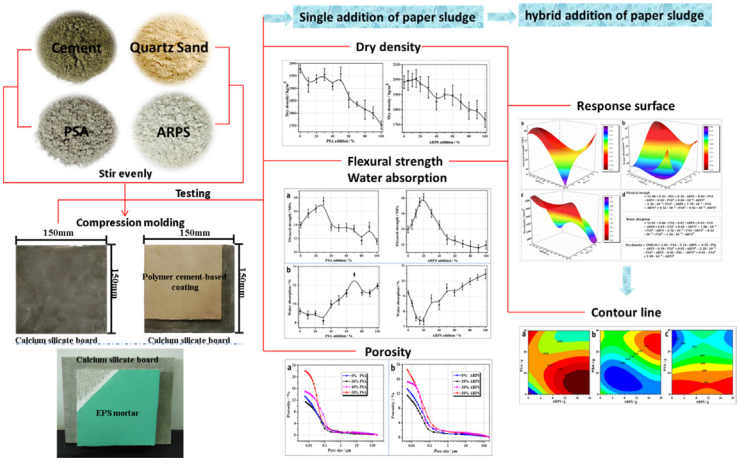

ARTICLE INFO

Article history:
Received 13 March 2018
Received in revised form 18 August 2019
Accepted 1 September 2019

Keywords:
Paper sludge powder
Calcium silicate board materials
Response surface methodology
Flexural strength
Water absorption

ABSTRACT

Calcium silicate board materials (CSBM), as a new environmental friendly and energy-saving building material, have been widely used in the construction of ceiling and insulation panel. This study aims to investigate the feasible utilization of two kinds of paper sludge powder, paper sludge ash (PSA) and alkali recovery paper sludge (ARPS), as the supplementary materials to develop a sustainable CSBM with low water-cement ratio. The experimental results indicate that single addition of 30% PSA or 20% ARPS can improve the flexural strength of CSBM effectively because a moderate addition of paper sludge can decrease the porosity. Meanwhile, the addition of PSA or ARPS notably reduces the thermal conductivity of the CSBM and DSC-TG analysis present a better thermal stability before 650 °C. Furthermore, the reinforcing capability of the hybrid PSA/ARPS to CSBM is investigated using response surface methodology (RSM). In conclusion, the utilization of paper sludge powder presents a great potential to develop sustainable and energy-saving CSBM with enhanced flexural strength and reduced water absorption.

* Corresponding authors.
E-mail addresses: lingchao_lu@163.com (L. Lu), chengxin@ujn.edu.cn (X. Cheng).

https://doi.org/10.1016/j.conbuildmat.2019.116874
0950-0618/

1. Introduction

Energy sustainability and waste management have been the two major challenges worldwide [1,2]. Cement and concrete, as the most widely used construction building materials, are produced around 4200 million metric tons every year and most of them have been consumed for buildings [3,4]. Although these building materials are regarded as one of the major component leading to the energy crisis due to the large consumption of natural resources [4–6], it has a great potential to develop the sustainability of civil infrastructures by optimizing the functionalization of cementitious materials or mixed with other wastes produced from metallurgical plant or water treatment factory, achieving the energy sustainability and improving the waste management [7–8].

Paper sludge [9–11], as a by-product of the wastewater treatment, usually can be divided into two categories based on whether it contains fiber or not. It was reported that 30 million tons of paper sludge were generated every year and mainly utilized in landfill application in China. Some of them were even burned directly, which led to serious environmental pollution. Therefore, how to handle with these large amounts of paper sludge has become a worldwide challenge in the waste management and environmental remediation. Nowadays, the development of alternative cementitious materials by incorporating paper sludge rapidly grows. For example, Cusidó et al. [12] studied the influence of paper sludge on the properties of clay brick and revealed that paper sludge benefited to improve the thermal and acoustic insulation of the clay mixture, but reduced its mechanical strength. Frías et al. [13] analyzed the feasibility on the application of paper sludge in cement-based materials as a supplementary material, suggesting that the replacement rate of paper sludge can up to 30–55% in blended concrete with enough mechanical strength. Most of previous research indicated that the partial replacement of cement-based materials by paper sludge not only reduces the greenhouse emission during the fabrication of cement, but also lowers down the management costs of paper sludge. Although the addition of paper sludge has a negative effect on the mechanical properties of cement-based material, it can be used as an efficient alternative materials to develop the environmental friendly and sustainable construction and building materials in terms of waste recycling and management.

Calcium silicate board materials (CSBM), as a new environmental friendly building material [14,15], has been rapidly developed because it not only inherits all the functions of the traditional gypsum board, but also has superior performances in thermal/sound insulation, water resistance, mechanical strength and fire proof [16,17]. As a result, CSBM has been widely used in construction of ceiling and partition, roof of warehouse and thermals insulation panel of the wall. CSBM is usually made of by mixing three major components, cement as calcium materials, reactive quartz sand as siliceous materials and (wood) fibers as reinforcing materials, and fabricated by advanced producing technology of molding pressure, high-temperature autoclaved curing and other special technical processing [18,19]. The major hydration product, tobermorite ($Ca_5Si_6O_{17}·5H_2O$), plays an important role in the engineering properties of CSBM [20–22].

Extensive research has been conducted to investigate the fabrication and properties of CSBM. Lin et al. [23] studied the structural properties of cold-formed steel wall frame of CSBM and found that the failure mostly occurred at the bottom track of wall specimens due to the large deformation or tearing failure of track. Hamilton and Hall [24] investigated the packing effect and pore structure of CSBM and indicated that a randomly orientated open packing of acicular crystals led to the fine pore structure of CSBM, rather than the tubiform pores in a sintered matrix as in flame-proof materials. In addition, Chi et al. [25] investigated the influence of curing temperature on the microstructure and thermal conductivity of CSBM and revealed that the thermal conductivity of two kinds of CSBMs with different densities at room temperature decreased by 5% after exposure to 1000 °C for 4 h, but a slight increase in thermal conductivity was observed when the temperature decreased to 400 °C. However, previous research did not refer to: (1) the relationship between the physical (dry density and water resistance) and mechanical properties of CSBM; (2) how to decrease the production cost of CSBM; and (3) how to fabricate sustainable and lightweight CSBM satisfying the requirement of JC/T 564.1-2008 [26].

In this paper, the effects of paper sludge powder on the properties of CSBM were investigated. Firstly, the CSBM was prepared by using ordinary Portland cement (OPC), quartz sand (QS) and two kinds of paper sludge powder, paper sludge ash (PSA) and alkali recovery paper sludge (ARPS). Secondly, the influence of single addition of PSA or ARPS on the physical properties (dry density and water absorption), flexural strength and thermal conductivity of CSBM was experimentally studied and optimized to satisfy the criteria as per JC/T 564.1-2008, as shown in Table 1. Finally, the hybrid addition of PSA/ARPS composites was optimized using response surface methodology (RSM) to develop a sustainable CSBM [27–29], which has better strength than that modified by single addition of PSA or ARPS.

2. Experimental procedures

2.1. Raw materials

Portland cement clinker (42.5 grade) was used as the main binder and calcareous materials to prepare the CSBM, and the superfine quartz sand (SiO_2 content > 95%) was used as high temperature stability agent and siliceous materials, which can improve the mechanical strength through the pozzolanic reaction with $Ca(OH)_2$. Two types of paper sludge powder, PSA and ARPS, were obtained from the Huatai Company (Shandong Province, China). PSA is the calcination production of paper sludge with plentiful wood fiber under 750–1400 °C and ARPS is generated

Table 2
Chemical components of paper sludge/%.

Components	CaO	SiO_2	Al_2O_3	MgO	Fe_2O_3	TiO_2	SO_3	Others
PSA	49.2	17.2	15.9	0.9	1.2	0	14.3	1.3
ARPS	91.3	2.1	0.5	3.5	0.3	0.1	0.4	3.2

Table 1
JC/T 564.1-2008 standard for different type of CSBM.

Performance	I	II	III	IV	In this study
Dry density/g/cm^3	≤0.95	0.95 < D ≤ 1.2	1.2 < D ≤ 1.4	>1.4	1.7 < D ≤ 2.0
Water absorption/%	–	–	–	–	<8
Flexural strength/MPa	5	6	8	9	>14
Thermal conductivity/W/(m K)	≤0.20	≤0.25	≤0.30	≤0.35	≤0.25

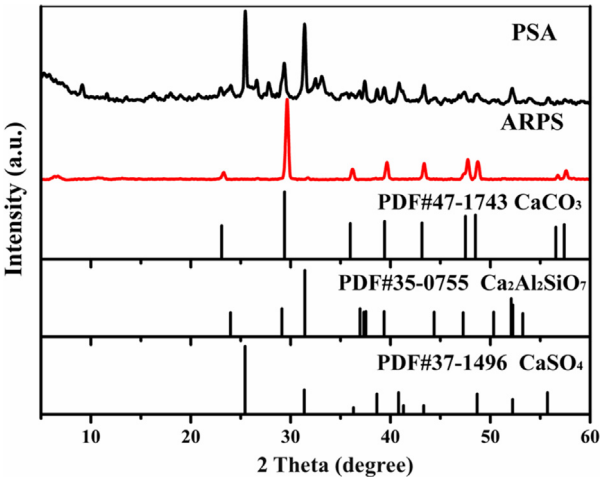

Fig. 1. XRD patterns of the PSA and ARPS.

from the causticizing reaction in papermaking process. Chemical components of the PSA and ARPS are shown in Table 2. Fig. 1 shows the XRD patterns of the PSA and ARPS, and based on the PDF database, PSA mainly consists of $CaSO_4$ and $Ca_2Al_2SiO_7$, located around the 2θ of 25° and 31°, respectively. However, $CaCO_3$ is the major component of ARPS due to the strong diffraction peak located around the 2θ of 29.5° and 48°.

2.2. Specimen preparation

The Ca/Si ratio of the CSBM used in this study was set as 1.22 based on our previous research [30], and the morphology of tobermorite under the appropriate Ca/Si ratio is shown in Fig. 2. The mix proportions of the CSBM are shown in Table 3 and it should be noted that the content of paper sludge is by the weight of CSBM. The flow chart of the fabrication and characterization of the CSBM is shown in Fig. 3(a). The detailed preparation procedures of the CSBM are as follows:

1) Cement clinker was firstly mixed with quartz sand and paper sludge powder at the water to cement (w/c) ratio of 0.2 for 5 min;
2) The fresh mixtures were cast using compression moulding method under the pressure of 40 MPa, and then transferred to an autoclaved container with the temperature of 190 °C for 6 h;
3) The specimens were quickly cooled down to about 50 °C using an electric fan;
4) The CSBM was obtained after dried at 40 °C for 12 h in a vacuum dryer.

2.3. Testing methods

The differential distribution and cumulative volume of raw materials were investigated by a laser particle size analyzer (LPSA13320, USA). The water absorption and dry density of the CSBM were measured as per GB/T 7019-2014 [31]. The specimens were kept in a vacuum drying oven at 105 ± 5 °C until changes in mass no longer occurred before the test. In addition, flexural strength of the CSBM was conducted using a universal testing machine (CMT5504, MTS) with maximum capacity of 50 KN at a loading speed of 0.3 kN/s. Morphology of the tobermorite in the CSBM was obtained using a field emission scanning electron microscope (FESEM, FEI, QUANTA FEG 250). X-ray diffractometer (XRD, Bruker D8-Advance, Cu Kα target, λ = 1.5406 Å) was used to qualitatively identify mineralogical phases through comparing the standard diffraction patterns. The porosity of specimens was determined by a mercury intrusion porosimetry (MIP, Quantachrome, AutoProe 9500 IV). Thermal conductivity was tested using an intelligent thermos-conductivity machine (DRL-III, Xiangke company, CHN). The differential scanning calorimetry (DSC) and thermogravimetric (TG) curves were collected by a simultaneous thermal

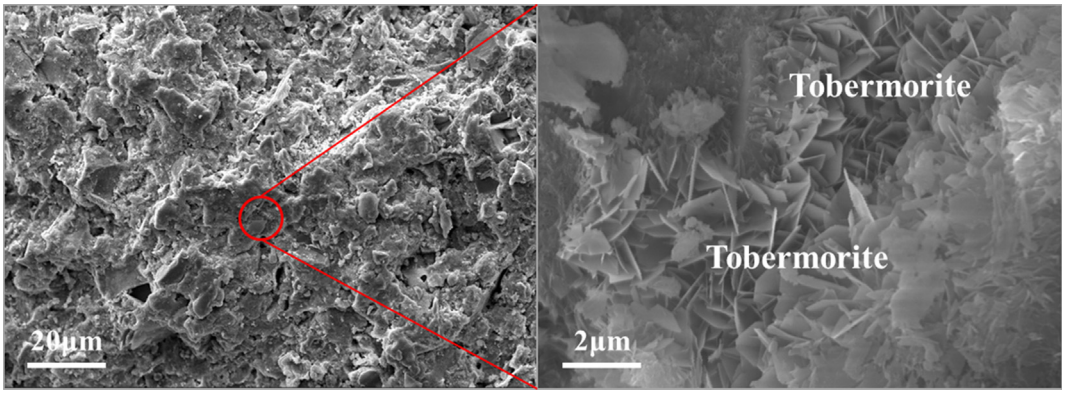

Fig. 2. Morphology of tobermorite under the Ca/Si ratio of 1.22.

Table 3
Mix proportions of the CSBM with paper sludge.

Components	CSBM (wt. %)		Paper sludge (wt. %)		W/C ratio
	OPC	QS	PSA	ARPS	
CSBM-PSA	72	28	0–100	0	0.2
CSBM- ARPS	72	28	0	0–100	0.2

Note: paper sludge is by the weight of CSBM.

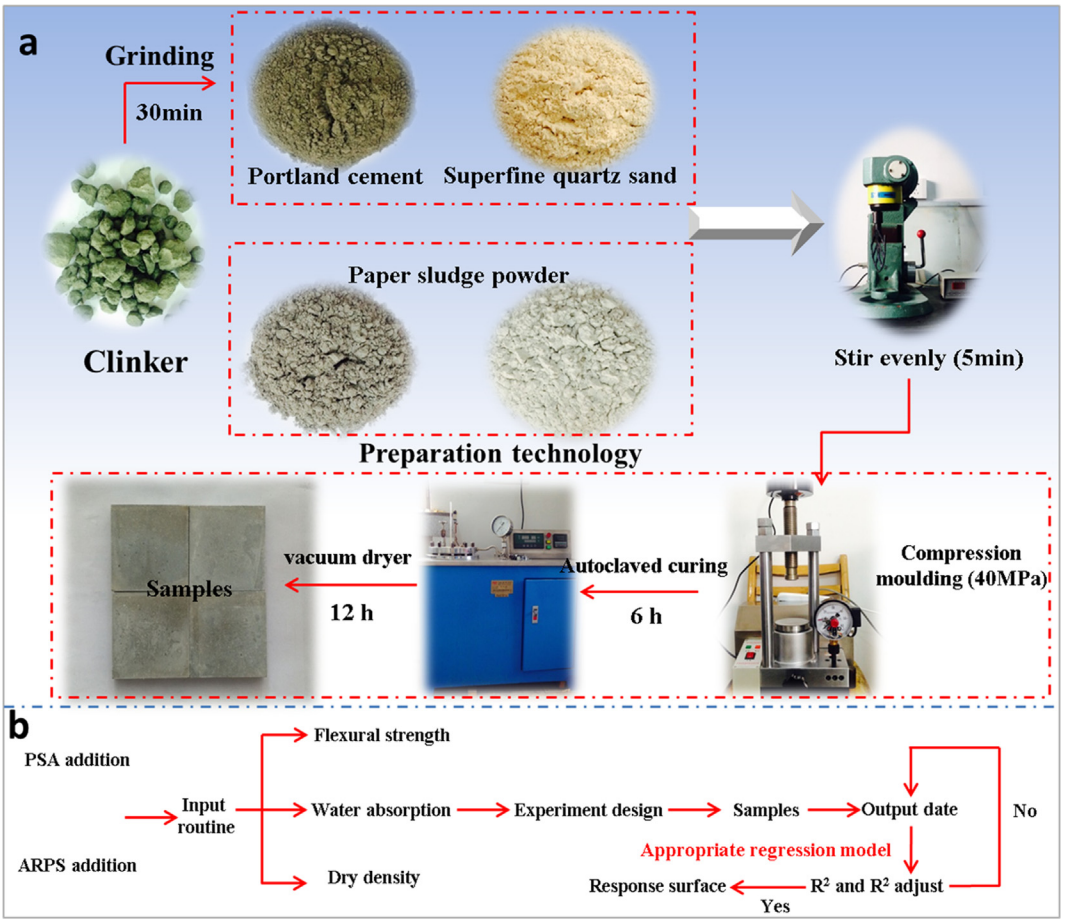

Fig. 3. (a) Flow chart of the fabrication and characterization of the CSBM and (b) the schematic diagram of RSM.

analysis instrument (TGA 1600HT METTLER TOLEDO) at heating rate of 10 °C/min under argon environment.

2.4. RSM design

Response surface methodology (RSM) is a kind of mathematical and statistical technique that has widely been used for optimizing multiple parameters and predicting the responses through the surface model [32,33]. In this paper, two parameters (the hybrid addition of PSA and ARPS) in the CSBM were optimized using RSM with the model of optimal experimental design, which is a flexible design structure to accommodate custom models and minimize the number of runs [34,35]. Runs are determined by a selection criterion chosen during the build. In optimal design, 16 runs (i.e., mix design) are used for independent variables. Schematic diagram of RSM is shown in Fig. 3(b). The appropriate regression model adopted by R^2 and R^2 adjust (determination coefficient) is shown in Table 4. All determinations coefficient of different properties in the cubic model are larger than 0.95, presenting that the variables are closely related to properties and the equation is as follows:

Table 4
Determinations coefficient for the responses.

Response	Flexural strength	Water absorption	Dry density
R^2	0.987	0.995	0.998
R^2 adjusted	0.968	0.988	0.995

$$\mathbf{y}(\mathbf{x}) = \boldsymbol{b}_0 + \sum_{i=1}^{n} \boldsymbol{b}_i \boldsymbol{x}_i + \sum_{i<}^{n} \sum_{j}^{n} \boldsymbol{b}_{ij} \boldsymbol{x}_i \boldsymbol{x}_j + \sum_{i=1}^{n} \boldsymbol{b}_{ii} \boldsymbol{x}_i^2 + \sum_{i=1}^{n} \boldsymbol{b}_{ii} \boldsymbol{x}_i^3 + \sum_{i\neq}^{n} \sum_{j}^{n} \boldsymbol{b}_{ijj} \boldsymbol{x}_i \boldsymbol{x}_j^2 + \sum_{i<}^{n} \sum_{j<}^{n} \sum_{k}^{n} \boldsymbol{b}_{ijk} \boldsymbol{x}_i \boldsymbol{x}_j \boldsymbol{x}_k + \varepsilon \quad (1)$$

where $\mathbf{y}(\mathbf{x})$ is the response, $\boldsymbol{x}_i$, $\boldsymbol{x}_j$ and $\boldsymbol{x}_k$ are the parameters, $\boldsymbol{b}$ is the regression coefficient, $\boldsymbol{n}$ is the number of parameters included in the experiment, and ε is the random error.

3. Results and discussion

3.1. CSBM modified by single addition of PSA or ARPS

The mechanical strength of the CSBM is usually decided by two factors, the generation of tobermorite and the interior structure of the samples. The interior structure of the CSBM may be reflected by the porosity, water absorption and dry density, and the flexural strength can present the toughness of the CSBM and predict the yield of tobermorite. Furthermore, the formation process of tobermorite in the CSBM is shown in Fig. 4.

Dry density is usually regarded as the important parameter to evaluate the water resistance, compactness and workability of the CSBM. Fig. 5 shows the effect of single addition of PSA or ARPS on the dry density of CSBM. It reveals that the dry density of CSBM generally decreases with the increasing amount of paper sludge powder due to the lightweight of PSA (1495 g/cm^3) and ARPS (1279 g/cm^3). Since the lowest dry density of the CSBM modified

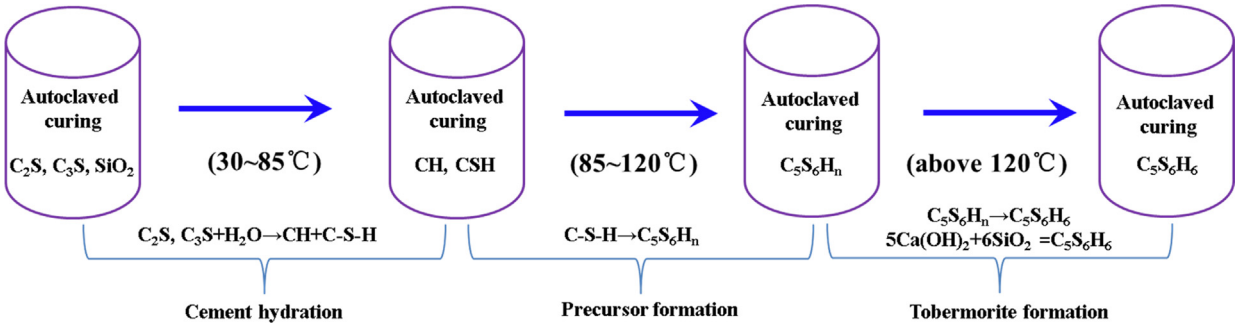

Fig. 4. The formation process of tobermorite in the CSBM.

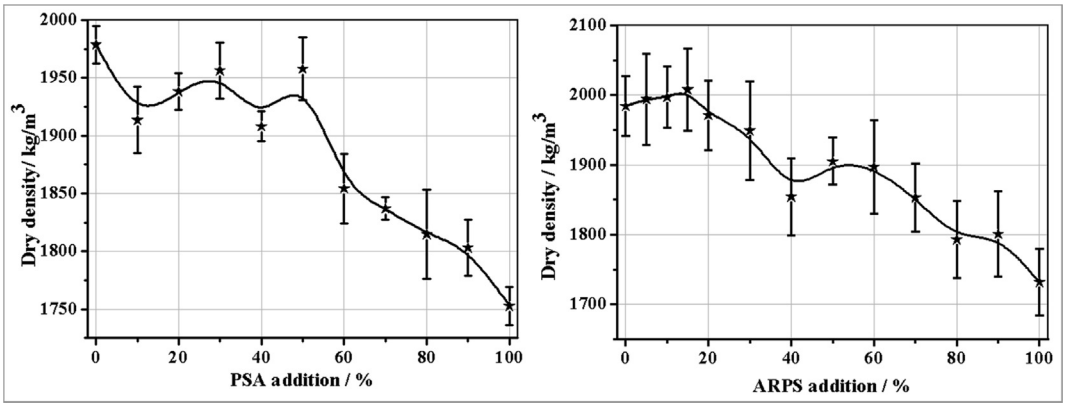

Fig. 5. Effect of single addition of PSA or ARPS on the dry density of CSBM.

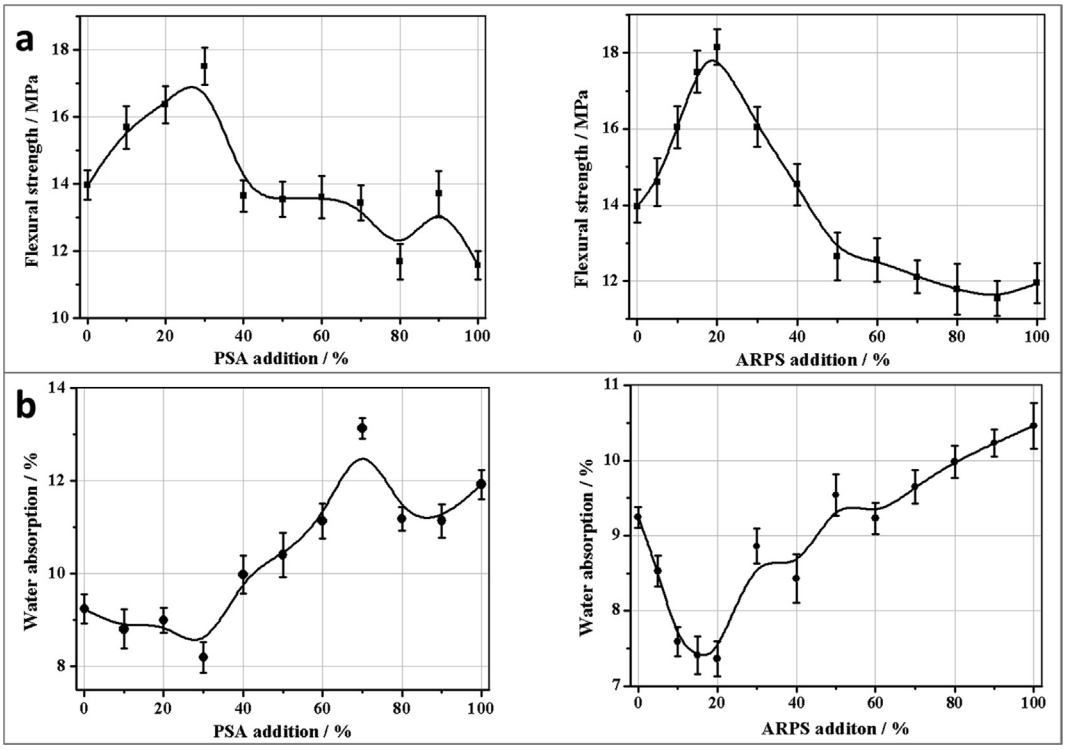

Fig. 6. Effect of single addition of PSA or ARPS on (a) the flexural strength and (b) water absorption of CSBM.

by PSA or ARPS is higher than 1.7 g/cm^3, which belongs to the type of IV listed in Table 1, the following parameters, including water absorption, flexural strength and thermal conductivity, should be optimized to satisfy the criteria of IV.

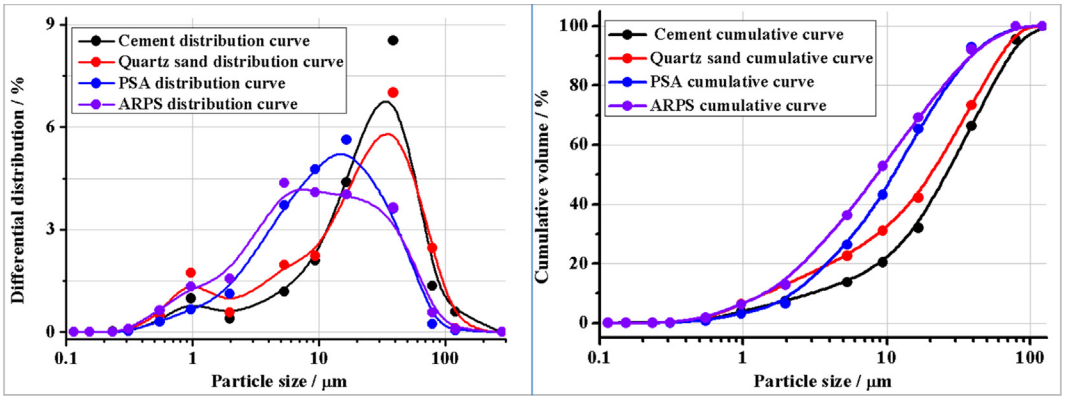

Fig. 7. The differential distribution and cumulative volume of PSA and ARPS particles compared to that of cement and quartz sand.

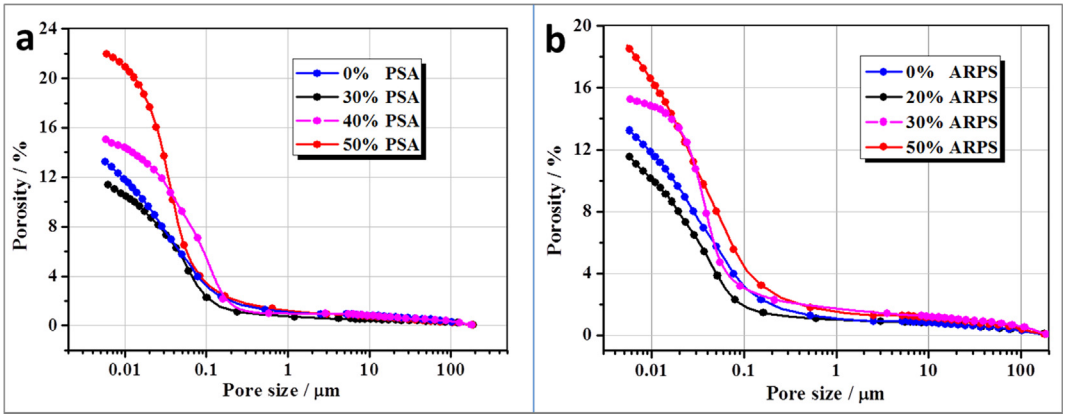

Fig. 8. The porosity of CSBM with different amount of (a) PSA (b) ARPS.

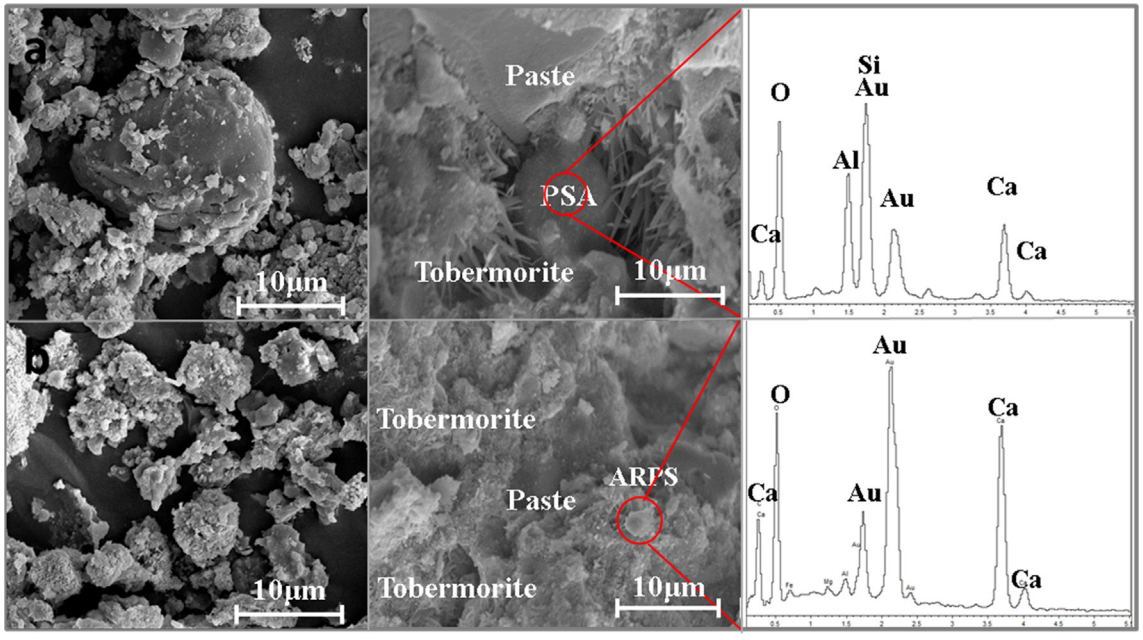

Fig. 9. SEM images EDX analysis of CSBM with (a) PSA and (b) ARPS.

Fig. 6 shows the flexural strength and water absorption of the CSBM with different amount of PSA (CSBM-PSA) or ARPS (CSBM-ARPS). Fig. 6(a) indicates that flexural strength of the CSBM firstly increases but then decreases with the increasing amount of each component. The reason is that the filling effect of PSA and ARPS particles to cement plays an important role in improving the

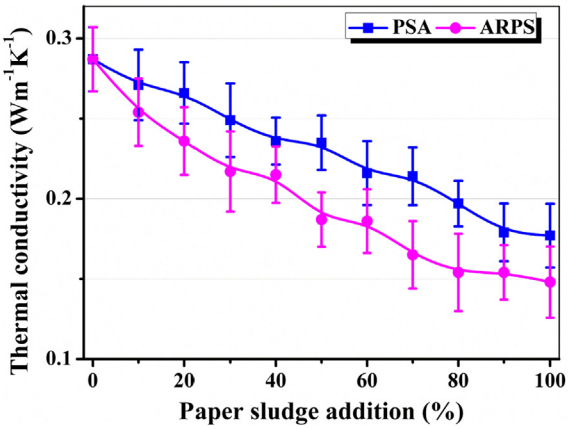

Fig. 10. The thermal conductivity of CSBM with different amount of PSA and ARPS.

flexural strength of CSBM, because both of them are chemical inertia. The differential distribution and cumulative volume of cement, quartz sand, and PSA and ARPS particles are investigated by LPAS, as shown in Fig. 7. It indicates that the particle size of cement ranging from 10 μm to 50 μm, is similar to that of quartz sand, but larger than that of PSA and ARPS (5 μm to 50 μm). The smaller size of PSA and ARPS can fill the pores in the cement and therefore densify the matrix, which contributes to improve the mechanical properties of CSBM [36].

In order to confirm this point, the porosity of CSBM with different amount of PSA and ARPS was conducted using MIP, as shown in Fig. 8. The results indicate that the porosity of CSBM can be lowered down to 11.7% and 11.9% by incorporating 30% PSA and 20% ARPS, respectively. Furthermore, Fig. 9 shows the microstructures of the CSBM modified by PSA and ARPS. It is clear to see that PSA and ARPS particles fill in the gaps among the tobermorite and uniformly distribute in the CSBM matrix, indicating that the filling effect of PSA and ARPS to cement matrix. However, further increasing amount of each component can dramatically increase the porosity of CSBM due to the decreased amount of cementing material. More importantly, no matter how much PAS or ARPS is added, flexural strength of the CSBM is always higher than the criteria value (9 MPa) described in IV in Table 1, indicating that the utilization of paper sludge powder can satisfy the mechanical requirement IV of the CSBM. According to the principle of highest strength, 30% addition of PSA or 20% addition of ARPS can significantly improve the flexural strength of CSBM to 16.9 MPa or 18.2 MPa, which is almost two times that of the criteria value. However, since the water absorption is usually negative correlated with the mechanical behaviour of CSBM, there is no doubt that it

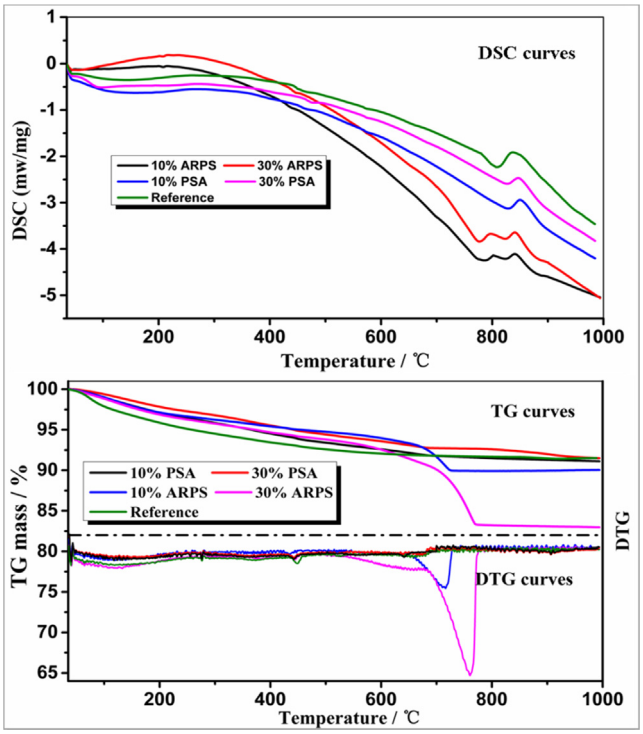

Fig. 12. DSC and TG curves of the CSBM with different addition of paper sludge powder.

firstly decreases and then increases with the increasing amount of each component, as shown in Fig. 6(b). Since the water absorption of CSBM is expected to be decreased as low as possible, the optimum single addition of PSA and ARPS should be limited in 30% and 20%, which can reduce the water absorption of the CSBM from 9.24% to 8.21% and 7.35%, respectively.

Fig. 10 shows the thermal conductivity of the CSBM with different addition of paper sludge powder. It indicates that the single addition of PSA or ARPS notably reduces the thermal conductivity of the CSBM because thermal conductivity t of PSA (0.168 W/m K) and ARPS (0.066 W/m K) are lower than that of CSBM, 0.287 W/m K, and the addition of ARPS obviously contributes more to the reduction of thermal conductivity of the CSBM. As seen from Fig. 10, it indicates that 30% addition of PSA or 20% addition of ARPS can significantly reduce the thermal conductivity from 0.287 W/m K to 0.249 W/m K or 0.236 W/m K, respectively, which also satisfies the requirement IV of thermal conductivity described in Table 1.

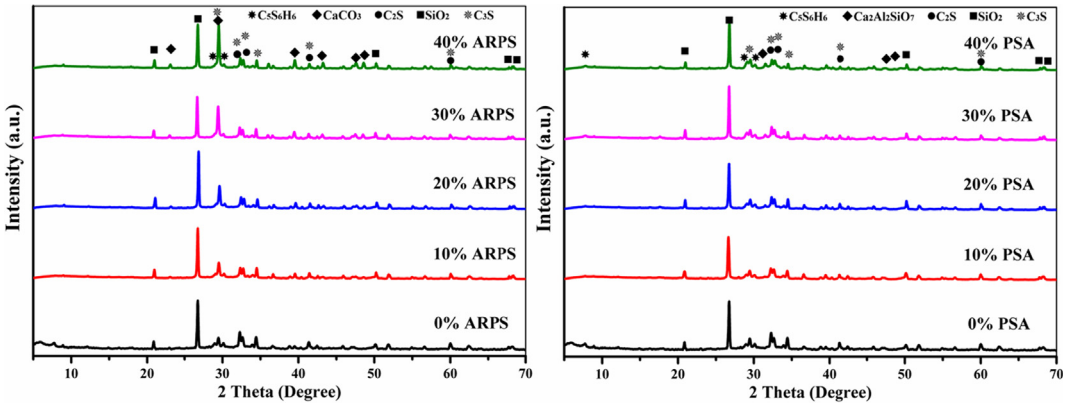

Fig. 11. XRD patterns of CSBM with different addition of PSA and ARPS.

Table 5
Experimental design and responses by RSM.

Run No.	A :PSA/g (Actual/Coded)	B: ARPS/g (Actual/Coded)	Y1: Flexural strength/MPa	Y2: Water absorption/%	Y3: Dry density/kg/m^3
1	0/-1	20.0/1	17.6	9.5	1987
2	0/-1	6.0/-0.4	15.4	10.1	1970
3	9.2/-0.39	0/-1	15.5	9.8	1961
4	16.1/0.07	20.0/1	16.8	12.9	1928
5	6.5/-0.57	13.8/0.38	18.0	9.4	1971
6	17.1/0.14	11.3/0.13	16.3	11.7	1931
7	30.0/1	20.0/1	15.0	13.0	1882
8	17.1/0.14	11.3/0.13	16.4	11.3	1932
9	30.0/1	12.0/0.2	15.1	12.5	1921
10	17.1/0.14	11.3/0.13	16.4	11.5	1934
11	23.4/0.557	5.6/-0.444	15.6	11.5	1901
12	0/-1	6/-0.4	15.8	10.2	1977
13	10.2/-0.318	6.5/-0.346	16.7	9.0	1963
14	9.2/-0.39	0/-1	15.9	9.8	1960
15	30.0/1	0/-1	17.8	12.4	1869
16	30.0/1	0/-1	17.6	12.5	1868

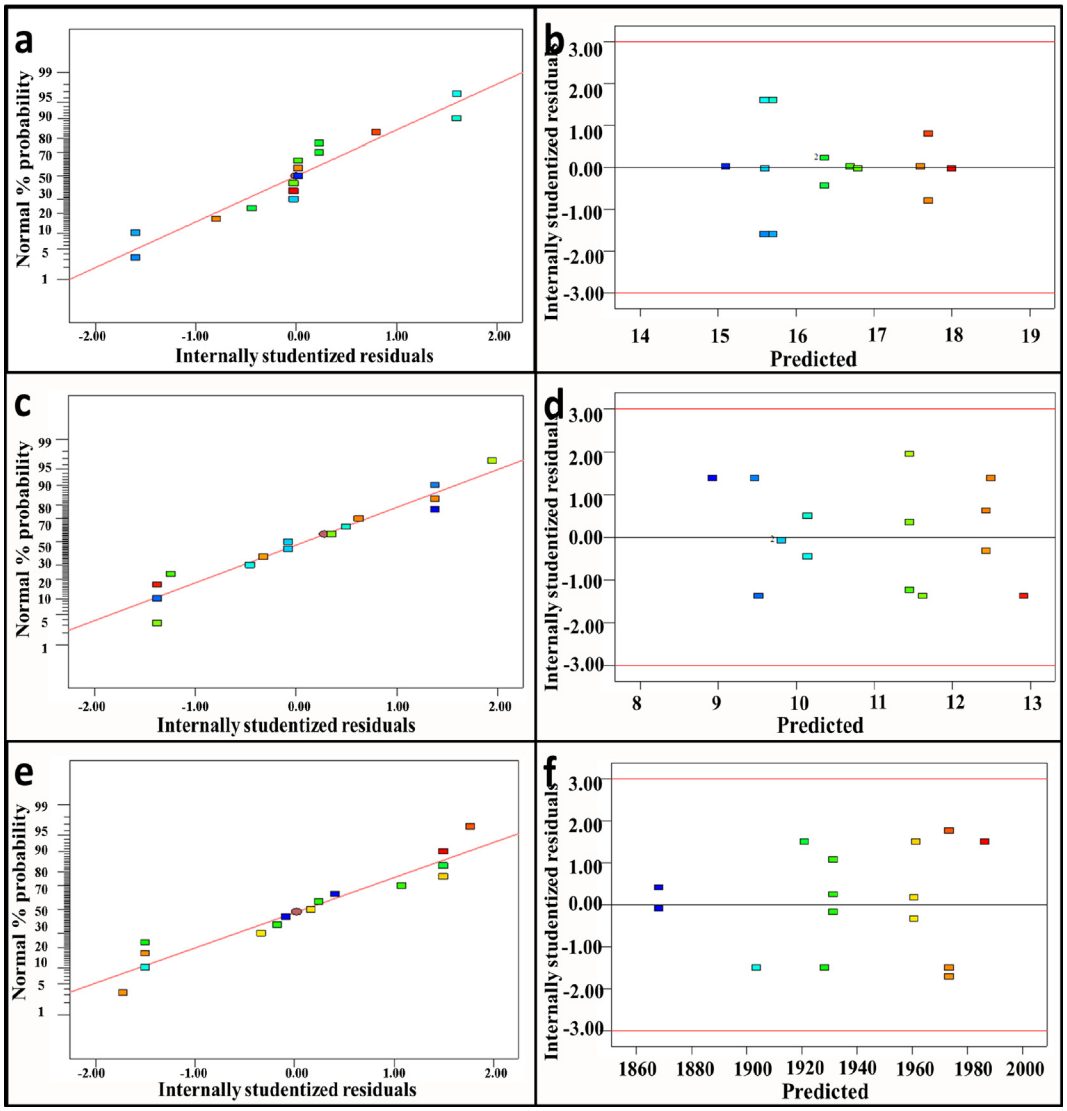

Fig. 13. (a) (c) and (e) Normal probability plots for the residuals of flexural strength, water absorption and dry density (b) (d) and (f) Plot of residual vs. predicted response for flexural strength, water absorption and dry density.

In summary, based on the principle of higher flexural strength, lower water absorption and thermal conductivity, the optimum single addition of PSA or ARPS is 30% or 20%, which can improve the flexural strength by 21.0% or 30.3%, lower down the water

absorption by 11.1% or 20.5%, and decrease the thermal conductivity by 13.2% and 17.8%. All the three parameters satisfy the requirement IV described in Table 1.

3.2. XRD and DSC-TG analysis

Fig. 11 shows the XRD patterns of CSBM with different addition of PSA and ARPS, indicating that the diffraction peak of $CaSO_4$ from the PSA vanished due to the generation of ettringite (unconspicuous diffraction peak in the 2θ of 9). The obvious phenomenon from the XRD patterns is that the diffraction peaks of tobermorite become weak gradually with the increasing of PSA and ARPS, and chemical effects for the CSBM is negligible.

Since the CSBM without fiber is usually used as fire-proof materials for cement kiln and large warehouses due to the generation of tobermorite, which can ensure the materials for normal use in 650 °C, it should be confirmed that the CSBM modified by paper sludge powder in high temperature is thermally stable. Fig. 12 shows the DSC-TG curves of the CSBM with different addition of paper sludge. By comparing these curves, a small endothermic peak can be found from 410 °C to 430 °C, resulting from the decomposition of $Ca(OH)_2$ generated from the hydration of C_3S and C_2S. The endothermic peak of the CSBM-ARPS in the temperature range of 750–800 °C is likely due to the decomposition of $CaCO_3$ from paper sludge, and the exothermic peak from 800 to 830 °C may be due to the dehydroxylation of tobermorite. From the DTG and TG curves in Fig. 12, little weight loss can be found from 800 to 830 °C, indicating that this endothermic effect results from the breakdown of anhydrous tobermorite to an intermediate amorphous phase rather than the dehydroxylation of tobermorite. Therefore, it can be concluded that the CSBM, CSBM-ARPS and CSBM-PSA present a better thermal stability before 650 °C due to the little weight loss.

3.3. Response surface methodology (RSM)

The effects of PSA and ARPS on the properties of CSBM present huge distinction. Therefore, optimum hybrid addition of PSA and ARPS in CSBM can be obtained using RSM from the model of optimal experimental design. In this section, the thermal conductivity

Table 6
ANOVA for response surface cubic model.

Response	Source of data	Sum of squares	Degree of freedom	F-value	P-value > F-value
Flexural strength					
	Model	14.17	9	50.59	< 0.0001
	A-PSA	1.81	1	58.29	0.0003
	B-ARPS	0.26	1	8.41	0.0273
	AB	7.7	1	247.61	< 0.0001
	A^2	0.81	1	25.9	0.0022
	B^2	8.01E-03	1	0.26	0.63
	A^2B	6.16E-03	1	0.2	0.672
	AB^2	0.88	1	28.25	0.0018
	A^3	0.53	1	16.88	0.0063
	B^3	0.049	1	1.58	0.2558
	Residual	0.19	6		
	Lack of fit	1.88E-05	1	5.04E-04	0.983
	Pure error	0.19	5		
	R^2	0.987			
	Adj. R^2	0.968			
Dry density					
	Model	22105.16	9	305.25	< 0.0001
	A-PSA	1674.6	1	208.12	< 0.0001
	B-ARPS	0.93	1	0.12	0.7455
	AB	50.5	1	6.28	0.0462
	A^2	36.2	1	4.5	0.0782
	B^2	399.97	1	49.71	0.0004
	A^2B	16.85	1	2.09	0.198
	AB^2	750.57	1	93.28	< 0.0001
	A^3	502.52	1	62.45	0.0002
	B^3	9.01	1	1.12	0.3308
	Residual	48.28	6		
	Lack of Fit	18.11	1	3	0.1437
	Pure Error	30.17	5		
	R^2	0.998			
	Adj. R^2	0.995			
Water absorption					
	Model	28.08	9	141.93	< 0.0001
	A-PSA	5.51	1	250.55	< 0.0001
	B-ARPS	1.89	1	86.03	< 0.0001
	AB	2.28	1	103.88	< 0.0001
	A^2	0.35	1	15.87	0.0072
	B^2	1.91	1	86.95	< 0.0001
	A^2B	2	1	90.97	< 0.0001
	AB^2	0.092	1	4.18	0.0868
	A^3	1.74	1	79.08	0.0001
	B^3	0.41	1	18.82	0.0049
	Residual	0.13	6		
	Lack of Fit	0.042	1	2.33	0.1876
	Pure Error	0.09	5		
	R^2	0.995			
	Adj. R^2	0.988			

will not be researched due to the similar effects of PSA and ARPS, and obviously trends in previous work. Table 5 shows the detailed information on the experimental design and responses by RSM, indicating that the value of flexural strength, water absorption and dry density of the CSBM ranges from 15 to 18 MPa, 9 to 13% and 1868 to 1987 kg/m^3, respectively.

In order to verify the effectiveness of the model, the normal curves of residuals in RSM are plotted in Fig. 13. It should be pointed out that the term of residuals in RSM can reflect the compliance between the actual value, estimated value and estimated abnormal value in responses; however, the studentized residuals can be calculated from the residuals divided by the estimated standard deviation [37], which are more accurate to reflect the abnormal value, compared with the residuals standard deviation. As shown in Fig. 13(a) (c) and (e), it can be seen that residuals of the three parameters, flexural strength, water absorption and dry density, almost fall on a straight line, implying that the errors are normally distributed and no abnormal value in responses [38]. Furthermore, the residuals for the three parameters as a function of the predicted responses are plotted in Fig. 13(b) (d) and (f). The common pattern for plot of residual vs. predicted response is that the plot should be a random scatter, suggesting the variance of original observations is constant for all values of the response [39]. Since there are no obvious patterns in all cases, it can be deduced that the proposed model can well predict and optimize the three parameters used in the design of the CSBM. In addition, the influence of PSA, ARPS and hybrid PSA/ARPS on the dry density, water absorption and flexural strength of the CSBM is investigated by variance analysis (ANOVA) [40], and the results are shown in Table 6. P-value means the probability for variance of samples caused by sampling error, and F-value means the ratio of two variances. The smaller P-value and larger F-value stand for the high precision of the testing results. In terms of flexural strength, the ANOVA results indicate that the probability of P-value > F (P > F) is less than 0.0001, which confirms the model terms are significant. Besides, the Lack of Fit (LOF) of 0.983 implies that it is not significant relative to the pure error. Similar results can also be obtained for the water absorption and dry density. Therefore, it can be concluded that the model used for optimization of the two parameters, PSA and ARPS, is highly effective.

Figs. 14 and 15 show the response surface and contour line of actual factor for the flexural strength, water absorption and dry density of the CSBM. As shown in Figs. 14(a) and 15(a), the flexural strength significantly increases with the increasing hybrid addition of PSA/ARPS, and then presents roughly fluctuate when the PSA addition is higher than 10%. The optimal flexural strength of the CSBM should be achieved within the following domain, PSA from 0–12% with ARPS from 12–20%. The fitting Eq. (2) of flexural strength obtained by response surface is shown as follows. According to the RSM results, it can be seen that the optimal flexural strength of the CSBM can be achieved with the PSA addition of 5% and ARPS addition of 18%, At this time, the flexural strength goes up to highest value (18.26 MPa), which shows stronger reinforcement to CSBM than the single addition of PSA and ARPS.

In addition, Figs. 14(b) and 15(b) presents the effect of hybrid addition of PSA/ARPS on the water absorption of the CSBM, according to the fitting Eq. (3) as below. There also remains an optimal domain (ARPS of 2–14% and PSA of 2–13%) on the response surface. Water absorption of the CSBM even remains stable at the higher content (larger than 12%) of ARPS, due to the low water absorption of ARPS and another reason may be due to the decreasing porosity. However, the large amount of PSA can lead to an increase in water absorption of the CSBM due to the high water absorption of PSA itself. Thus, compared with ARPS, PSA plays a dominant role in the water absorption of the CSBM, and the water absorption reaches the lowest value (8.7%) when the hybrid addition of PSA and ARPS is 6% and 8%, which is lightly higher than the single addition.

Moreover, Figs. 14(c) and 15(c) shows the response surface and contour line of dry density based on the following fitting Eq. (4). It can be seen that dry density decreases with the increasing addition of PSA, and ARPS presents the reduced dry density only when the addition of PSA is in the range of 22–30%. Thus, PSA will play a dominant role in the dry density of the CSBM. Therefore, the

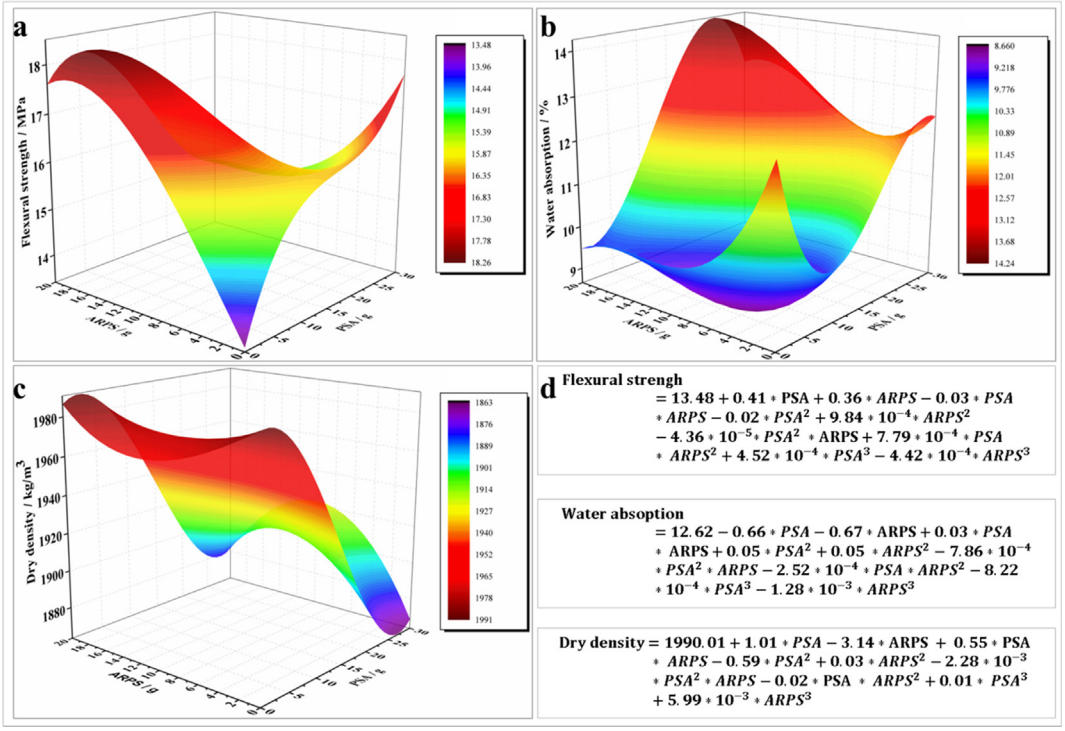

Fig. 14. The response surface and fitting equation of actual factor for the (a) flexural strength (b) water absorption and (c) dry density of CSBM.

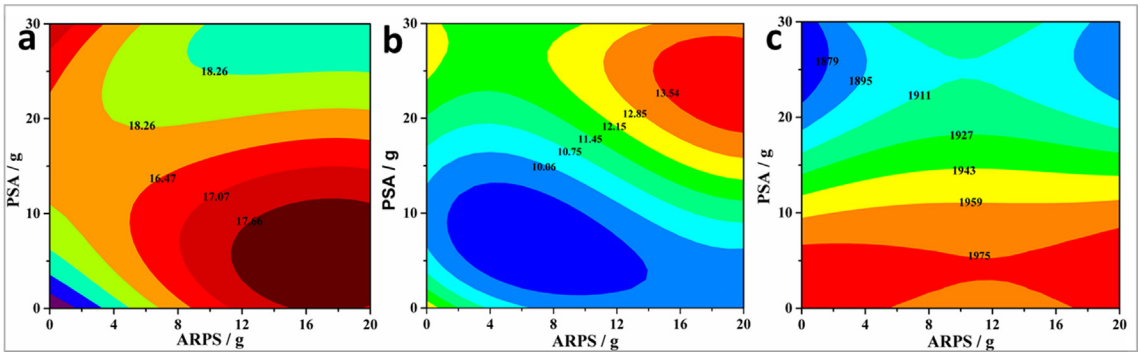

Fig. 15. The contour line of actual factor for the (a) flexural strength (b) water absorption and (c) dry density of CSBM.

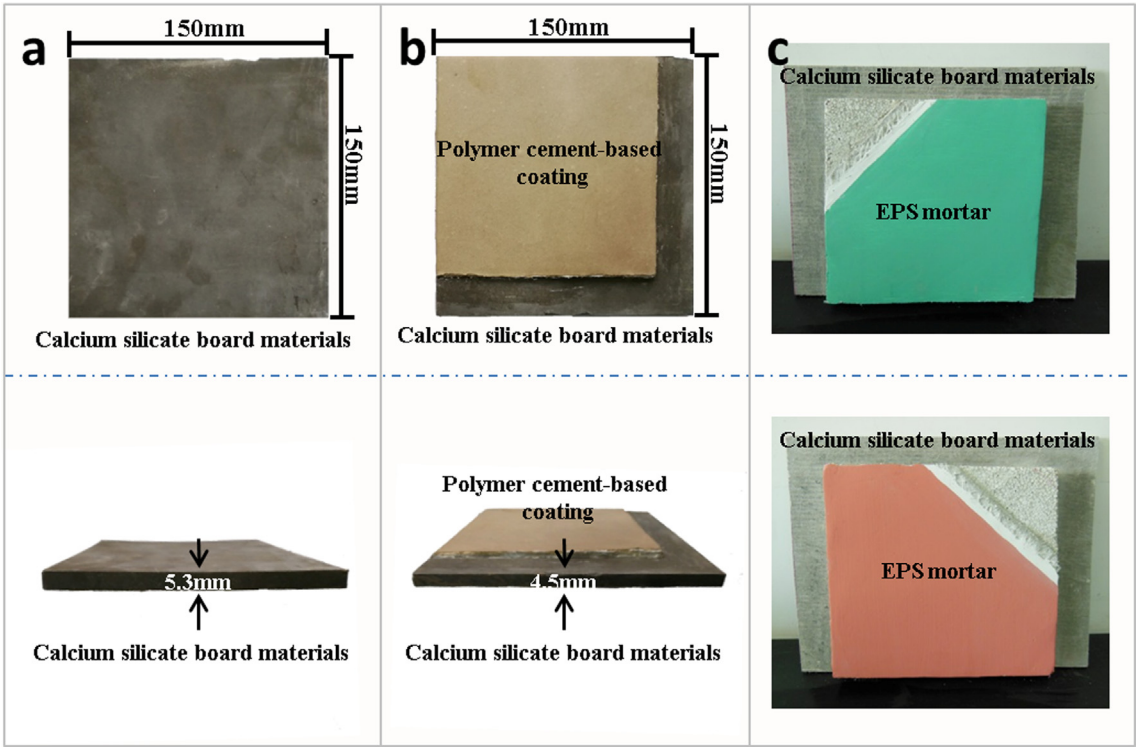

Fig. 16. The application of the CSBM with paper sludge in different areas (a) normal CSBM; (b) CSBM substrate with polymer/cement coating; (c) CSBM substrate with EPS mortar.

comprehensive comparison of RSM results for flexural strength, water absorption and dry density can reveal that the optimized hybrid addition of PSA (5%) and ARPS (18%) for the CSBM with highest flexural strength and lower water absorption.

$$\text{Flexural strength} = 13.48 + 0.41 \times \text{PSA} + 0.36 \times \text{ARPS} - 0.03 \times \text{PSA} \times \text{ARPS} - 0.02 \times PSA^2 + 9.84\times10^{-4} \times ARPS^2 - 4.36\times10^{-5} \times PSA^2 \times \text{ARPS} + 7.79 \times 10^{-4} \times \text{PSA} \times ARPS^2 + 4.52 \times 10^{-4} \times PSA^3 - 4.42\times10^{-4} \times ARPS^3 \quad (2)$$

$$\text{Water absoption} = 12.62 - 0.66 \times \text{PSA} - 0.67 \times \text{ARPS} + 0.03 \times \text{PSA} \times \text{ARPS} + 0.05 \times PSA^2 + 0.05 \times ARPS^2 - 7.86 \times 10^{-4} \times PSA^2 \times \text{ARPS} - 2.52 \times 10^{-4} \times \text{PSA} \times ARPS^2 - 8.22 \times 10^{-4} \times PSA^3 - 1.28 \times 10^{-3} \times ARPS^3 \quad (3)$$

$$\text{Dry density} = 1990.01 + 1.01 \times \text{PSA} - 3.14 \times \text{ARPS} + 0.55 \times \text{PSA} \times \text{ARPS} - 0.59 \times PSA^2 + 0.03 \times ARPS^2 - 2.28 \times 10^{-3} \times PSA^2 \times \text{ARPS} - 0.02 \times \text{PSA} \times ARPS^2 + 0.01 \times PSA^3 + 5.99 \times 10^{-3} \times ARPS^3 \quad (4)$$

3.4. Potential application of the CSBM modified by paper sludge powder

Due to the optimized properties, such as enhanced mechanical properties, reduced dry density, water absorption and thermal conductivity, the CSBM modified by paper sludge powder has a great potential to be used in many areas, such as thermal insulation wall, ceiling, partition and substrate board of polymer coating. Fig. 16 shows the potential application of CSBM modified by paper sludge powder. Fig. 16(a) shows the CSBM (150 mm * 150 mm) modified by PSA and ARPS, and Fig. 16(b) shows a product prepared by depositing a polymer/cement coating on the CSBM substrate

shown in Fig. 15(a). Furthermore, Fig. 16(c) indicates that CSBM can be used as the substrate for expanded polystyrene (EPS) mortar since CSBM has an enhanced flexural strength and lower thermal conductivity compared with the traditional substrate like plasterboard and fibreboard, and the final product is capable of better thermal insulation and reduced cost, and can be used in the area of ceiling or wall in buildings. In conclusion, the recycling of paper sludge has a great potential to develop the sustainable CSBM with enhanced properties, and benefits to the development of waste management and energy efficiency for infrastructure.

4. Conclusions

In this study, the influence of two kinds of paper sludge powder, paper sludge ash (PSA) and alkali recovery paper sludge (ARPS), on the properties of calcium silicate board materials (CSBM) was investigated. The single addition of PSA or ARPS was experimentally optimized and the hybrid addition of PSA/ARPS was determined by response surface methodology (RSM) for achieving sustainable CSBM. The main conclusions of this study are highlighted as below:

(1) The single addition of 30% PSA or 20% ARPS can improve the flexural strength of CSBM by 21.0% and 30.3%, reduce the water absorption by 11.3% and 16.7%, and lower down the thermal conductivity by 13.2% and 17.8%, respectively;
(2) With the increasing amount of PSA and ARPS, porosity of the CSBM decreases first and then increases again, and the lowest porosity of CSBM can be reduced to 11.7% or 11.9% by incorporating 30% PSA or 20% ARPS, respectively;
(3) The addition of PSA or ARPS notably reduces the thermal conductivity of the CSBM and DSC-TG analysis present a better thermal stability before 650 °C.
(4) RSM results reveal the hybrid PSA (5%)/ARPS (18%) composites lead to 30.8% increase in flexural strength, which shows stronger reinforcement to CSBM than the single addition, and the hybrid PSA (6%)/ARPS (8%) composites lead to 10.4% reduction in water absorption;
(5) The developed CSBM composites with paper sludge powder can satisfy the requirement as per JC/T 564.1–2008.

Finally, it can be concluded that the utilization of paper sludge powder has a great potential to develop lightweight CSBM with enhanced flexural strength and reduced water absorption, and benefits to the development of waste management and energy efficiency for infrastructure.

Declaration of Competing Interest

There are no conflicts of interest to this work.

Acknowledgements

This work is supported by 13th Five-Year the state key development program (2016YFC0701001), Natural Science Foundations of China (51602126 and 51672108), and postdoctoral program of University of Jinan (XBH1718).

References

[1] A. De Meyer, D. Cattrysse, P. Ostermeyer, J. Van Orshoven, Implementation of OPTIMASS to optimise municipal wastewater sludge processing chains: proof of concept, Resour. Conserv. Recycl. 114 (2016) 168–178.
[2] L. Coppola, D. Coffetti, E. Crotti, G. Gazzaniga, T. Pastore, An empathetic added sustainability index (EASI) for cementitious based construction materials, J. Clean. Prod. 220 (2019) 475–482.
[3] M. Usman, A.Y. Khan, S.H. Farooq, A. Hanif, S. Tang, R.A. Khushnood, S.A. Rizwan, Eco-friendly self-compacting cement pastes incorporating wood waste as cement replacement: a feasibility study, J. Clean. Prod. 190 (2018) 679–688.
[4] A. Joshaghani, M. Balapour, A.A. Ramezanianpour, Effect of controlled environmental conditions on mechanical, microstructural and durability properties of cement mortar, Constr. Build. Mater. 164 (2018) 134–149.
[5] L. Li, X. Zhou, Y. Li, C. Gong, L. Lu, X. Fu, W. Tao, Water absorption and water/fertilizer retention performance of vermiculite modified sulphoaluminate cementitious materials, Constr. Build. Mater. 137 (2017) 224–233.
[6] Z. Lu, B. Xu, J. Zhang, Y. Zhu, G. Sun, Z. Li, Preparation and characterization of expanded perlite/paraffin composite as form-stable phase change material, Sol. Energy 108 (2014) 460–466.
[7] Z. Lu, J. Zhang, G. Sun, B. Xu, Z. Li, C. Gong, Effects of the form-stable expanded perlite/paraffin composite on cement manufactured by extrusion technique, Energy 82 (2015) 43–53.
[8] L. Coppola, T. Bellezze, A. Belli, M.C.,, et al., Binders alternative to Portland cement and waste management for sustainable construction - part 2, J. Appl. Biomater. Funct. Mater. 16 (4) (2018) 207–221.
[9] S. Kim, H.J. Kim, J.C. Park, Application of recycled paper sludge and biomass materials in manufacture of green composite pallet, Resour. Conserv. Recycl. 53 (12) (2009) 674–679.
[10] P. Filiatrault, C. Camiré, J.P. Norrie, C.J. Beauchamp, Effects of de-inking paper sludge on growth and nutritional status of alder and aspen, Resour. Conserv. Recycl. 48 (3) (2006) 209–226.
[11] J.A.O. de Alda, Feasibility of recycling pulp and paper mill sludge in the paper and board industries, Resour. Conserv. Recycl. 52 (7) (2008) 965–972.
[12] J.A. Cusidó, L.V. Cremades, C. Soriano, M. Devant, Incorporation of paper sludge in clay brick formulation: ten years of industrial experience, Appl. Clay Sci. 108 (2015) 191–198.
[13] M. Frías, O. Rodríguez, M.S. De Rojas, Paper sludge, an environmentally sound alternative source of MK-based cementitious materials. A review, Constr. Build. Mater. 74 (2015) 37–48.
[14] M. Nithyadharan, V. Kalyanaraman, Experimental study of screw connections in CFS-calcium silicate board wall panels, Thin-Walled Struct. 49 (6) (2011) 724–731.
[15] A. Hamilton, C. Hall, A note on the density of a calcium silicate hydrate board material, J. Build Phys. 31 (1) (2007) 69–71.
[16] Y. Wang, Y.J. Chuang, C.Y. Lin, The performance of calcium silicate board partition fireproof drywall assembly with junction box under fire, Adv. Mater. Sci. Eng. 2015 (2015).
[17] M. Akao, A. Yamazaki, Y. Fukuda, Fungus resistance of vermiculite board and comparison to calcium silicate board and gypsum wall board, J. Mater. Sci. 39 (18) (2004) 5869–5872.
[18] M. Sakiyama, Y. Oshio, T. Mitsuda, Influence of quartz particle size and Ca/Si ratio on strength of autoclaved calcium silicate board, Inorg. Mater. 7 (2000) 278–284.
[19] I. Richardson, G. Groves, The structure of the calcium silicate hydrate phases present in hardened pastes of white Portland cement/blast-furnace slag blends, J. Mater. Sci. 32 (18) (1997) 4793–4802.
[20] J. Ding, Z. Tang, S. Ma, Y. Wang, S. Zheng, Y. Zhang, S. Shen, Z. Xie, A novel process for synthesis of tobermorite fiber from high-alumina fly ash, Cem. Concr. Compos. 65 (2016) 11–18.
[21] I. Maruyama, G. Igarashi, Y. Nishioka, Y. Tanigawa, Carbonation and fastening strength deterioration of calcium silicate board: analysis of materials collected from a ceiling collapse accident, J. Struct. Eng. 78 (689) (2013) 1203–1208.
[22] C. Yip, J. Van Deventer, Microanalysis of calcium silicate hydrate gel formed within a geopolymeric binder, J. Mater. Sci. 38 (18) (2003) 3851–3860.
[23] S.-H. Lin, C.-L. Pan, W.-T. Hsu, Monotonic and cyclic loading tests for cold-formed steel wall frames sheathed with calcium silicate board, Thin-Walled Struct. 74 (2014) 49–58.
[24] A. Hamilton, C. Hall, Physicochemical characterization of a hydrated calcium silicate board material, J. Build. Phys. 29 (1) (2005) 9–19.
[25] C.T. Do, D.P. Bentz, P.E. Stutzman, Microstructure and thermal conductivity of hydrated calcium silicate board materials, J. Build Phys. 31 (1) (2007) 55–67.
[26] JC/T 564.1-2008. Fiber reinforce calcium silicate boards, part I: Non-asbestos calcium silicate boards. Building Materials Standardization Administration of China, Beijing, China.
[27] Q. Li, L. Cai, Y. Fu, H. Wang, Y. Zou, Fracture properties and response surface methodology model of alkali-slag concrete under freeze–thaw cycles, Constr. Build. Mater. 93 (2015) 620–626.
[28] B.S. Mohammed, O.C. Fang, K.M.A. Hossain, M. Lachemi, Mix proportioning of concrete containing paper mill residuals using response surface methodology, Constr. Build. Mater. 35 (2012) 63–68.
[29] K.E. Alyamac, E. Ghafari, R. Ince, Development of eco-efficient self-compacting concrete with waste marble powder using the response surface method, J. Clean. Prod. 144 (2017) 192–202.
[30] M. Chen, L. Lu, S. Wang, P. Zhao, W. Zhang, S. Zhang, Investigation on the formation of tobermorite in calcium silicate board and its influence factors under autoclaved curing, Constr. Build. Mater. 143 (2017) 280–288.
[31] GB/T 7019-2014. Tests methods for fiber cement products. Standardization Administration of China, Beijing, China.
[32] C. Li, Q. Xiao, Y. Tang, L. Li, A method integrating Taguchi, RSM and MOPSO to CNC machining parameters optimization for energy saving, J. Clean. Prod. 135 (2016) 263–275.
[33] G. Campatelli, L. Lorenzini, A. Scippa, Optimization of process parameters using a response surface method for minimizing power consumption in the milling of carbon steel, J. Clean. Prod. 66 (2014) 309–316.

[34] M. Ranic, M. Nikolic, M. Pavlovic, A. Buntic, S. Siler-Marinkovic, S. Dimitrijevic-Brankovic, Optimization of microwave-assisted extraction of natural antioxidants from spent espresso coffee grounds by response surface methodology, J. Clean. Prod. 80 (2014) 69–79.
[35] P. Arun, S.M. Pudi, P. Biswas, Acetylation of glycerol over sulfated alumina: reaction parameter study and optimization using response surface methodology, Energy Fuels 30 (1) (2016) 584–593.
[36] K. Sun, X. Zhou, C. Gong, Y. Ding, L. Lu, Influence of paste thickness on coated aggregates on properties of high-density sulphoaluminate cement concrete, Constr. Build. Mater. 115 (2016) 125–131.
[37] B.K. Körbahti, M.A. Rauf, Determination of optimum operating conditions of carmine decoloration by UV/H2O2 using response surface methodology, J. Hazard. Mater. 161 (1) (2009) 281–286.
[38] A. Adebanjo, M.G. Kulkarni, A.K. Dalai, N.N. Bakhshi, Pyrolysis of waste fryer grease in a fixed-bed reactor, Energy Fuels 21 (2) (2007) 828–835.
[39] M. Zahid, N. Shafiq, M.H. Isa, L. Gil, Statistical modeling and mix design optimization of fly ash based engineered geopolymer composite using response surface methodology, J. Clean Prod. 194 (2018). S0959652618314987.
[40] A.I. Nassar, N. Thom, T. Parry, Optimizing the mix design of cold bitumen emulsion mixtures using response surface methodology, Constr. Build. Mater. 104 (2016) 216–229.